2019

Novel muscle contusion injury model and repair mechanism

BOSTON UNIVERSITY

SCHOOL OF MEDICINE

Thesis

NOVEL MUSCLE CONTUSION INJURY MODEL AND REPAIR MECHANISM

by

DANIELLE CORBIN

B.A., Lake Erie College, 2017

Submitted in partial fulfillment of the

requirements for the degree of

Master of Science

2019

Approved by

First Reader _____

Beth Bragdon, Ph.D.
Assistant Professor of Orthopaedic Surgery

Second Reader _____

Louis C. Gerstenfeld, Ph.D.
Professor of Orthopaedic Surgery

DEDICATION

For the pursuit of knowledge and application.

ACKNOWLEDGMENTS

I would like to thank Dr. Beth Bragdon for her phenomenal mentorship on this project, without her dedication this surely wouldn't have come together. Thanks also goes to Dr. Gerstenfeld for facilitating an amazing environment to teach and learn.

NOVEL MUSCLE CONTUSION INJURY MODEL AND REPAIR MECHANISM

DANIELLE CORBIN

ABSTRACT

This study investigates the skeletal muscle repair and regeneration process following blunt trauma injury in murine models. Skeletal muscle injury is recorded most often in sports injuries and include strains and sprains, contusions, and bruising, however, there is growing consensus about the role skeletal muscle plays in the reparative process of bone fractures. Skeletal muscle stem cells or satellite cells are mesenchymal stem cell derived cells that exist between the basal lamina and cell membrane of muscle fibers usually in close proximity to capillary beds. After a traumatic injury, satellite cells respond to the influx of signaling from immune cells, oxygen tension, and myogenic proteins which influence differentiation into myoblasts for repair of tissue damage. Research continues to elucidate the relationship between bone and skeletal muscle following trauma injuries. Skeletal muscle stem cells play a vital role in fracture healing, and in certain conditions, are even induced into the osteogenic pathway. The goals of this study are to characterize the temporal progression of myogenesis during muscle repair that will be used with future studies of muscle and bone injury. And to identify potential crosstalk mechanisms between muscle and bone repair during trauma.

In our experiment model trauma was introduced to mice with a modified muscle contusion device where a weight was dropped onto the femoral quadriceps muscles and the quadriceps and biceps muscle tissues were harvested at post-operative days (POD) 2, 4, 12, 16, and 24. Reverse-Transcriptase Quantitative Polymerase Chain Reaction was

used to analyze gene expression profiles for satellite/stem cells (*Pax7* and *Prx1*), muscle regeneration (*MyoD*, *Myf5*, *Myl2*, and *Myh1*), angiogenesis (*VegfA*, *VegfR2*), myokine (*Myostatin* and *IL6*), and BMP signaling (*ID1*).

Our findings indicate that both *Pax7* and *Prx1* expression slightly decreased after injury but showed a significant ($p<0.05$) increase and peak of expression at POD 16 in the femoral quadriceps muscles. The early myogenic genes, *MyoD* and *Myf5* peaked early at POD 4 while the adult myofiber markers, *Myl2* and *Myh2*, peaked later at POD 16 in the femoral quadriceps muscles. Only slight changes were observed in the femoral biceps muscles. The angiogenic genes peaked at POD16 in the femoral quadriceps muscles and POD 12 in the femoral biceps muscles. The expression of Myostatin, an inhibitor of muscle mass, decreased early (POD 4 and 12) however showed a non-significant increase at POD 16 in the femoral quadriceps muscles. Lastly, the expression of ID1, which is downstream target of BMP signaling peaked early at POD 4 in the femoral quadriceps muscles.

These data indicates that stem/satellite cells decrease in response to muscle injury but by POD 4, myogenic commitment and programming occurs. While early myogensis occurs, BMP signaling peaks and Myostatin expression decreases suggesting a coordinated event. Adult myofiber regeneration occurs in parallel to angiogenesis. The myogenic events were primarily isolated to the injured femoral quadriceps muscles. This model of muscle injury can be used to study muscle regeneration within context to bone injury.

TABLE OF CONTENTS

LIST OF TABLES

LIST OF FIGURES

LIST OF ABBREVIATIONS

AJSM……. American Journal of Sports Medicine

BMP 2……..…….Bone Morphogenetic Protein 2

ECM……...Extracellular matrix

FGF……..…… fibroblast growth factor

HGF……...Hepatocyte growth factor

HSF……..... Hepatocyte-stimulating factor

ID-1…….. DNA-binding protein inhibitor

IGF-1……..Insulin-like growth factor 1

IL-6……Interleukin-6

MSTN…….. Myostation

Myf5……. Myogenic factor 5

Myh1……..….Myosin-1; striated muscle myosin heavy-chain

Myl2……. Myosin light chain 2

MyoD……Myogenic differentiation

Pax 3……..Paired box protein 3

Pax 7……. Paired box protein 7

PECAM-1…….……Platelet endothelial cell adhesion molecule

POD…… Post-operative days

Prx1/Prrx1……..….Paired related homeobox 1

RANKL-κβ…….….Receptor activator of nuclear factor κβ

RT-qPCR…….Real Time Quantitative Polymerase Chain Reaction

TGF-β……. Transforming growth factor β

(TNF-α)……...….Tumor necrosis factor – α

VegF-A……..……. Vascular endothelial growth factor A

VegfR2…….……Vascular endothelial growth factor R2

VML…….. Volumeric muscle loss

INTRODUCTION

Skeletal muscle is the most abundant tissue in the human body constituting close to 40% of the total human body mass. Muscle injury and damage can stem from many origins and range from pathological conditions to acute trauma. Skeletal muscle injuries are the most common sports-related injuries (Boage et al., 2012) among athletes and include lacerations, strains, and contusions. Soft tissue trauma is also common among industrial workers and clinically manifest in localized pain, swelling, reduced range of motion and tenderness to palpation (Singh et al., 2017). Degenerative musculoskeletal disorders, which can be caused by ischemia or neurological pathologies, also provide pressing incentive to further comprehend the physiological mechanisms and factors surrounding muscle regeneration and repair. The purpose of this study is to investigate the mechanisms of muscle repair following blunt trauma in murine models. Isolating muscle injury and repair processes from complex musculoskeletal injuries will provide a context for understanding muscle injury repair mechanisms and crosstalk to bone during repair and regeneration.

Development of Skeletal Muscle, Satellite Cells, and Pax 7

Skeletal muscle and connective tissue of vertebrates develop from the mesoderm germ layer and neural crest during embryogenesis. A germ layer is primary layer of cells that form during the early stages of embryo growth. The mesoderm can be divided into the paraxial, intermediate, and lateral mesoderm from the midline

position. During the third week of embryogenesis the mesoderm undergoes somitogenesis, where paired cell swellings (somites) appear from the rostral to caudal end of the embryo, on the paraxial mesoderm (lateral to the neural groove). Somite regions differentiate into dermamyotome (dermal and muscle components) and sclerotome (vertebral column component). The central dermamyotome region contains Pax7 positive progenitor cells that will develop into skeletal muscle (Relaix et al., 2005). Cells derived from this region continue to differentiate based on cell signaling and gene expression and eventually splits into a dermatome (contributes to the connective tissue of the neck, skin, and fat) and a myotome. Myotomes then differentiate into myoblasts which give rise to the myofibers that form skeletal muscle (Yin et al., 2013), and at this point they cannot reenter the cell cycle or regenerate themselves in any capacity. Myotome cells can also remain as a proliferating reserve cells in the muscle mass. These prenatal mesenchymal stem cells continue to migrate and differentiate throughout the embryo. In late-stage fetal development these reserve cells adopt their satellite cell positioning (Relaix et al., 2005). Satellite cells exist between the basal lamina and cell membrane of myofibers. Satellite cells are the myogenic progenitor cells of post-natal muscle, it is common belief that satellite cells self-repopulate through asymmetrical division, where one cell differentiates into a myoblast and the other continues to proliferate or become quiescent in response to damage (Zammit et al., 2006, Relaix et al., 2006).

Pax 7 and is a protein member of the Pax gene family that acts as a transcription factor with a paired box/homeodomain binding domain. Pax 3 is a

paralogue of Pax 7 and also plays a key role in the specification of cells that enter the myogenic program. Pax 3 is critical for delamination and migration of muscle precursors from somites to the appendages (Olguin et al., 2007). In the Pax 3/Pax 7 knockout, mice show major deficits in skeletal muscle development and cessation of myogenesis in late embryonic development (Relaix et al., 2005, Kansal et al., 2019). Pax 3 expression is down-regulated in satellite cells before birth. In Pax 7 homogenous knockouts, mice have no gross muscle defects though adult skeletal muscles have a receding number (Relaix et al., 2005) or completely devoid of satellite cells (Olguin et al., 2007). Pax 7 mutant mice also show reduced muscle growth, increased muscular atrophy, and extreme deficit in muscle regeneration after injury (Olguin et al., 2007). In vitro, Pax 7 expression is lower in recently activated proliferating satellite cells and is rapidly down regulated in cells that are committed to terminal differentiation. The role of Pax 7 is therefore paramount to satellite cell specification, survival, and renewal and hereby vital to skeletal muscle repair and regeneration.

Paired related homeobox 1 (Prx 1 or Prrx1) is a transcription factor expressed prenatally during limb bud formation and plays a significant role in craniofacial bone development. Postnatal cells derived from Prx1 cells are at the center of bone homeostasis and fracture repair (Wilk et al., 2017) because inactivation of key osteogenic factors such as RANKL (receptor activator of nuclear factor) κB ligand or BMP-2 (bone morphogenetic protein 2) expression in these cells causes osteopetrosis ("stone bone") and low-bone-mass phenotypic bones respectively (Wilk et al., 2017).

Post-natal cells expressing Prx 1 have been shown in culture to differentiate into osteoblasts and chondroblasts and thus, their properties suggest that cells expressing Prx 1 can be used to mimic and characterize the behavior of skeletal muscle stem cells (Wilk et al., 2017).

Muscle Injury Pathobiology

According to the American Journal of Sports Medicine, skeletal muscle follows three consecutive steps from injury to repair and this repair process remains consistent regardless of the cause (strain, contusion, or laceration) of injury. It is however dependent on many other cell types including macrophages, satellite cells, fibrocyte/adipocyte precursors, interstitial connective tissue, and endothelial cells for angiogenesis (Hardy et al. 2016).

The first phase is destruction, which is characterized by the rupture and necrosis of skeletal muscle fibers, hematoma formation between muscle stumps, and inflammatory cell response (Figure 2) (Järvinen et al., 2005).

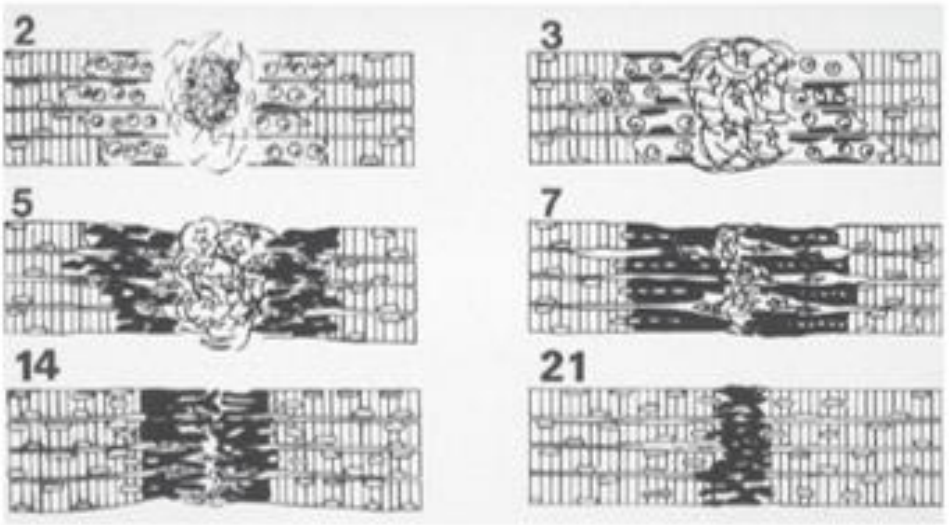

Figure 1: Skeletal Muscle Healing Schematic. This image illustrates how skeletal muscle repairs and regenerates itself after suffering an injury. **Day 2:** The necrotized parts of the transected myofibers are being removed by macrophages while, concomitantly, the formation of the connective tissue scar by fibroblasts has begun in the central zone. **Day 3:** Satellite cells have become activated within the basal lamina cylinders in the regeneration zone. **Day 5:** myoblasts have fused into myotubes in the regeneration zone, and the connective tissue in the central zone has become denser. **Day 7:** The regenerating muscle cells extend out of the old basal lamina cylinders into the central zone and begin to pierce through the scar. **Day 14:** the scar of the central zone has further condensed and reduced in size, and the regenerating myofibers close the central zone gap. **Day 21:** the interlacing myofibers are virtually fused with little intervening connective tissue (scar) in between. Modified from Järvinen, Tero AJSM 2005

Neutrophils begin invasion within an hour of injury and release proteases to aid with degrading cellular debris (Tidball, 2005). The concentration of neutrophils can remain elevated for up to 5 days. Within hours of injury the torn blood vessels allow polymorphonuclear leukocytes to relocate to the site of injury, and become monocytes that eventually become macrophages. The macrophages remove necrotic factors and work in tandem with fibroblasts to secrete growth factors, cytokines, and chemokines (Baoge et al., 2012). Satellite cells become active within 18 hours due to chemical stimulus and will participate in myofiber remodeling and repair process. The tissue damage also releases growth factors from the extracellular matrix (ECM) of

myofibers which initiates signal cascades. These factors include fibroblast growth factor (FGF) which stimulate and inhibit satellite cell differentiation, insulin-like growth factor-1 (IGF-1), insulin-like growth factor-2 (IGF-2) which solely stimulate differentiation, transforming growth factor-β (TGF-β) which stimulates collagen deposition, hepatocyte growth factor (HGF), tumor necrosis factor-α (TNF-α), and interleukin-6 (IL-6) which can activate the myogenic precursor, the satellite (stem) cell (Boage et al., 2012). Interleukin 6 (IL-6) is a cytokine released by metabolically active skeletal muscle. IL-6 has pleiotropic effects; stimulating B cells, hematopoietic stem cells, and hepatocytes due to its structural similarity to hepatocyte-stimulating factor (HSF) and hybridoma/plasmacytoma growth factor (HPGF) (Forcina et al., 2018). Skeletal muscle produces increased IL-6 during exercise which acts locally and in the circulation increasing muscle glucose uptake, angiogenesis, lipolysis, and muscle hypertrophy. Excess IL-6 is correlated with muscle atrophy and muscle wasting. Interleukin 1 (IL-1) is a master pro-inflammatory cytokine that lowers the pain threshold in many tissues (Dinarello et al., 2012). There are two IL-1 genes in circulation, an alpha and beta, that both bind to the same IL-1 receptor which is present in nearly all cells. Due to its role in numerous pathological conditions (rheumatoid arthritis, traumatic knee injuries, osteomyelitis, etc.) most research studies focus on ways to dampen the effects of IL-1. IL-1 exists in membrane fragments known as apoptotic bodies which are active in inducing neutrophil infiltration through inflamed or damaged blood vessels (Dinarello et al., 2012). IL-1 also extends neutrophil survival and contributes to the unique behaviors of activated neutrophils.

Phase two is the repair phase and is categorized by phagocytosis of the necrotized tissue, regeneration of myofibers, production of a connective tissue scar, and capillary infiltration to the injured area (Järvinen et al., 2005). Activated satellite cells proliferate and differentiate into new myoblasts that fuse to the injured myofibers, filling the gap created by the injury/phagocytosis. Repair is also executed by the formation of connective tissue by fibrin and fibronectin from the hematoma that formed during phase one. The scar tissue is essential in giving the muscle strength to withstand contractions while providing an anchoring site for fibroblasts to infiltrate the granulated tissue (Baoge et al., 2012). Dense scar tissue results from the excessive proliferation of the fibroblasts which interferes with the repair and regeneration process. Dense connective tissue may lead to incomplete functional recovery of the injured muscle during the remodeling phase.

The third phase is remodeling. It is characterized by the maturation of myoblasts into myofibers and the reorganization and strengthening of the scar tissue through contractions. During this phase, the muscle is expected to return to functional capacity (Järvinen et al., 2005).

Satellite Cells and Differentiation

A muscle fiber is a multinucleated cell that develops from multiple myoblasts that fuse into a myotube. The myotubes continues to grow and produce proteins that will help aid in its ability to become contractile. Myosin light chain- 2 (Myl 2 or MLC-2) is a protein in the sarcomere of muscles that binds calcium and contributes to the contractile property of muscle (Sheikh et al., 2015). Myosin heavy chain (Myh 1 or MHC) is an ATP-dependent motor protein that also contributes to the contractile abilities of the sarcomere and thus skeletal muscle.

Cells that initially enter the myogenic lineage depend on signaling created by the expression of myogenic determination factor (MyoD) gene family. The Myf 5 gene is also a member of the myogenic determination gene family which regulates cell cycle withdrawal and induction of differentiation of skeletal muscle fibers (Kitzmann et al., 1998). Satellite cells give rise to a population of myogenic precursor cells that express Pax 7 in addition to MyoD and Myf 5. Myogenic precursor cells later exit the cell cycle and enter terminal differentiation and fuse to form new myofibers (Latroche et al., 2017).

The somatic cell cycle consists of five stages: Growth 1 (G1), Synthesis (S), Growth 2 (G2), Mitosis (M), and Growth 0 (G_0) or "naught". All nucleated cells progress through the cell cycle during embryological development and differentiation. Genomic expression dictates when specific cell types "enter" (G1 through M) and "leave" (G_0) the cell cycle.

In the process of repairing damaged skeletal muscle, satellite cells produce proliferating myoblasts that have unique gene expressions in relation to MyoD and Myf 5. Myo D peaks at mid-G1, has a minimum during G1/S, increases again during S to M and is absent during G_0. (Kitzmann et al., 1998) Conversely, Myf 5 protein is high in the G_0 stage and decreases during G1 before increasing again towards the end of G1, remaining consistent until mitosis (reminder: skeletal muscle cells are multinucleated cells that undergo the mitotic division of the nucleus without cytokinesis -the division of the cytoplasm-).

Bone Morphogenetic Protein (BMP) is a member of the TGFβ signaling pathway and contributes to post-natal development of skeletal muscle, and satellite cells. The BMP family also plays a leading role in inducing osteoblast differentiation in multiple cell types. BMPs are growth factors involved in tissue structure throughout the body. Congenital BMP2 provides signaling to mesenchymal cells for proper differentiation into muscle, fat, cartilage, and bone (Rogers et al., 2015). BMP2 signaling has a ubiquitous role in the development of mesenchymal derived tissues. The role that BMP2 signaling plays in adult muscle tissue is still under investigation.

Skeletal Muscle Angiogenesis

Angiogenesis is the process of forming capillaries from existing blood vessels, and it plays a vital role in normal bodily function and all three phases of muscle repair and regeneration. Skeletal muscle is highly vascularized with microvascular units comprising of 5-10 capillaries between 3-4 adjacent myofibers (Latroche et al., 2017).

Angiogenesis regulation follows a controlled circuit; if the metabolic needs of the muscle tissue are not being met by the microcirculatory environment, the mechanical stress on the capillary lumen exerts an upstream effect on the capillaries to proliferate. Muscle fibers and endothelial cells respond to hyperemia, elevated tissue strain, or excessive contraction/relaxation by translating gene expression profiles which alter the endothelial cell phenotype which lead to capillary growth (Olfert et al., 2016). Capillary growth involves a legion of signaling molecules including vasodilators nitrous oxide (NO), prostaglandins, and adenosine. NO is credited with stimulating vascular endothelial growth factor (VEGF) expression under skeletal muscle stress (Olfert et al., 2016). VEGF-A is a proangiogenic mitogen factor in skeletal muscle that promotes post-natal capillary formation in exercised, overloaded, and stretched muscles. VEGF-A increases vascular permeability and VEGF-A deficient mice lose their angiogenic ability in skeletal muscle (Olfert et al., 2016, Uchida et al., 2015).

Cadherin 5 (Cdh5 or vascular endothelial cadherin (VE-cadherin)) is a vascular endothelial protein in cell-cell junctions that exists in a complex with two other proteins, vascular endothelial growth factor receptors (VEGFR-2) and platelet endothelial cell adhesion molecule (PECAM-1). Together, this complex transduces signals related to flow-dependent vasodilation, blood vessel remodeling, and atherosclerosis (Conway et al., 2017). VE-cadherin's role in flow sensation involves PECAM-1's activation of kinases that phosphorylate a key tyrosine in the junctional complex. The tyrosine can now interact with a polarity protein that can activate

inflammatory signaling in areas with turbulent flow and enhance flow dependent vascular remodeling (Conway et al., 2017).

After a traumatic event, satellite cells accumulate and proliferate near capillaries where they are stimulated by various growth factors secreted by endothelial cells (Singh et al., 2017). The proliferating satellite cells stimulate endothelial cells to form nascent capillaries and microvascular fragments (Singh et al., 2017). The number of capillaries surrounding a myofiber positively correlate with the number of satellite cells associated with the same myofiber (Latroche et al., 2017), and after injury, endothelial cells stimulate myogenic precursor cell growth and myogenic precursor cells exhibit angiogenic properties (Latroche et al., 2017).

Use of Growth Factors for Muscle Regeneration

It is possible to aid muscle regeneration with different biological growth factors. Injecting recombinant bFGF-6 (basic fibroblast growth factor) to the site of injury at the soleus muscle of adult mice can accelerate the differentiation of myotubes. (Armand et al., 2003). IGF-1 can also increase the efficiency of regenerating myofibers at two weeks post injury, and increase myofiber size at four weeks post injury (Takahashi et al., 2003), and even prevent age related muscle mass loss. However, IGF-1 may also lead to an increase in fibrosis due to the collagen stimulating and collagenase prohibiting properties of IGF-1. When IGF is injected in healthy old men loss of muscle mass typical with aging was prevented, however, due to the collagen simulating and collagenase prohibiting properties of IGF, there was an

increase in the development of fibrosis (Huard et al., 2002). bFGF-6 and IGF-1 both improve muscle performance, and even increase the number of regenerating myofibers by a factor of 3.5 (Kasemkijwattana et al., 1998). When HGF (50 ng) was injected into muscles on the day of injury, cells analyzed a day later showed a three-fold increase in MyoD positive cells compared to control muscle cells. HGF was also shown to increase the number of myogenic precursor cells, though that showed no improvement of the regeneration process (Miller et al., 2000). Combined we see how HGF effects the stem cell activation and differentiation.

Biologics and growth factors can be used to modulate remodeling with minimal scaring being the most successful outcome during the remodeling phase. The fibrotic tissue is regulated by TGF-β1 in both animals and humans (Chan et al., 2005) and has become a target for inhibition. Two drugs that have successfully inhibited of TGF-β1 are suramin and decorin (Chan et al., 2005; Nozaki et al., 2008). Suramin is an antiparasitic and antitumor drug that binds competitively to the TGF-β1 receptor. There are minor effects when injected less than 7 days post injury but injury fibrosis decreased with high dose injection 14 days after injury. Suramin treated groups also showed a dose-dependent increase in regenerating myofibers. Once healed, suramin injected muscles were stronger than control muscles (not dose-dependent) and showed less fibrosis and overall better healing. Decorin is a protein member of the small leucine-rich proteoglycan (SLRP) gene family and has a broad binding repertoire that encompasses matrix structural components including collagens, growth factors in the TGF-β family (Neill et al., 2012). Injection of decorin 10 to 15 days post injury

significantly deceased total fibrosis and enhanced the regeneration of injured muscle in a dose-responsive fashion with no observed side effects (Fukushima et al., 2001).

Soft Tissue Damage and Ectopic Bone Formation

In the adult, damaged muscle cells are repaired or replaced by a derivative of multipotent mesenchymal stem cells (MSC's) (Davis et al., 2015). Osteoblasts (secrete bone matrix), adipocytes, and chondrocytes are some of the cell lineages that originate from mesenchymal stem cells (Dunn et al.). Soft tissue injury healing plays a leading and vital role during the bone regeneration process (Davis et al., 2015). It has become more apparent that skeletal muscle is capable of providing osteoprogenitor cells to damaged periosteal tissue, and that muscular osteoprogenitor cells have similar potential to cells that are derived from the periosteum (Davis et al., 2015). In clinical cases of severe soft tissue injury, bone fracture healing is impeded compared to fractures with intact soft tissue. This poses a challenge for surgeons when facing crushed tissue or high energy trauma injuries which is quantified by the Gustilo-Anderson open fracture classification scale. This scale heavily focuses on skeletal muscle and vascular damage with higher grade injures associated with higher risk of complications (Hacking). The relationship between successful skeletal muscle repair and regeneration and bone regeneration and remodeling has proven to be unavoidable.

Fracture repair consists of three consecutive phases: a reactive phase, a reparative phase, and a remodeling phase. The reactive phase lasts less than a week, and is characterized by the initial fracture, hematoma formed from torn vasculature,

the infiltration of immune cells (lymphocytes, polymorphonuclear cells, and monocytes), and the recruitment of fibroblasts to form granulation tissue (Marsell and Einhorn., 2011). Granulation tissue also plays a role in secreting cytokines that initiate osteogenic differentiation of MSC's and promote angiogenesis (Einhorn and Gerstenfeld., 2015). The reparative phase of healing begins days after the reactive phase and lasts a few weeks. In this stage pluripotent MSC's respond to local oxygen levels and strain and differentiate into fibroblasts, chondroblasts, or osteoblasts (Davis et al., 2015). Bone healing occurs through a direct intramembranous ossification method or an indirect combination of intramembranous and endochondral ossification methods. Intramembranous ossification involves lamellar bone regeneration and fixation for stabilization, while endochondral ossification begins with a fibrocartilage epicenter that is subsequently replaced by a bony callus and woven bone deposition (Marsell and Einhorn., 2011, Gerstenfeld et al., 2006). In the years following the fracture the bone enters the remodeling phase, where woven bone is replaced by lamellar bone which is gradually remodeled due to mechanical stress.

Skeletal muscle is now known to have roles in aiding fracture repair through assisting in callus formation. During the reparative phase of bone regeneration, the interface between muscle and bone has the densest formed callus suggesting that muscle is a contributor to ectopic bone formation (Davis et al., 2015). BMP's are a family of growth factors involved in osteoblast differentiation and in the presence of BMP-2 cells derived from muscle are capable of expressing bone markers and forming bone (Gao et al., 2014). Muscle derived stem cells driven to osteogenic differentiation

can also give rise to chondrocytes and their potential for differentiation may rival their bone marrow equivalent (Gao et al., 2014). Skeletal muscle satellite cells are not limited to the myoblast lineage, and have showed osteogenic potential in numerous conditions. Following treatment with BMP's, satellite cells have differentiated in osteocytes both *in vivo* and *in vitro* when also treated with platelet-rich plasma, and have also been observed expressing both myoblastic and osteoblastic markers (Davis et al., 2015). Satellite cells are capable of spontaneously differentiating into osteoblasts as seen in the pathological condition fibrodysplasia ossificans progressiva, where muscle tissue becomes bone due to a mutation in BMP receptors. The impressive capability of satellite cells also has great potential for engineering treatment where bone marrow or the periosteum is compromised. Myogenic cells with MyoD expression contribute to fracture repair but are not found in the developing callus if the fracture allowed the periosteum to remain intact. Conversely, when the periosteum is damaged myogenic cells can act as a secondary supply of osteoprogenitor cells (Shah et al., 2013). This close relationship between muscle and bone is further extended through studies that show the density of bone is diminished with muscle disuse atrophy, denervation, or immobilization proving the importance of the mechanical relationship between bone and muscle (Davis et al., 2015).

Methods of Muscle Injury in Study

There are multiple models of muscle injury to use for the investigation of muscle repair mechanisms. Some of the most common methods are freeze, barium chloride, injected toxins (notexin and cardiotoxin), and physical injury (irradiation,

crush, and denervation) (Hardy et al., 2016). The repair mechanisms for each model is different as demonstrated by the different response of satellite cells and gene expression observes during repair for each model of injury.

The freezing muscle injury model destroys up to 96% of satellite cells in addition to the basal lamina and vasculature, and the regeneration process is much slower than the other methods, where there is only a 40% satellite cell decrease seen for other injury methods. The regeneration process is also much slower than with the freezing model compared to other models, but provides the only opportunity for researchers to observe infiltration of a muscular dead zone post injury (Hardy et al., 2016). Muscular dead zones bear similarity to volumetric muscle loss (VML) injuries characterized by military personnel. There is a complete loss of elements that contribute to muscle regeneration in VML injuries making recovery an unlikely possibility, and the remaining fibrosis and chronic loss of function progressively worsens over time (Hurtgen et al., 2016). VML injuries are also shown to delay fracture healing due to the disruptive effects on immune cell response.

Freeze injured muscle is the only method to see a complete return of satellite cells after a month long period, other methods see cycling of the stem cell population (actively processing through the cell cycle) three months after initial injury. The cardiotoxin model of muscle injury induced a dramatic increase of 20% in satellite cell number at just one-month post injury compared to injury models with barium chloride, notexin, and freeze injury. The number of satellite cells continued to increase 3-fold at three months post injury compared to the non-injured muscle. Inflammatory cells

remained elevated a month after injury with notexin and freeze injury models, while returning to baseline in cardiotoxin and barium chloride models.

Other considerations for the use of muscle trauma models is that none of the injury methods produced damage so significant that satellite cells were unable to recover (Hardy et al., 2016). Chemical models of injury use toxins that must be injected into the muscle of interest. However, toxins may not be distributed thoroughly throughout the muscle and therefore the targeted tissue will not be damaged and further analysis will be skewed (Hardy et al., 2016).

The method of injury is selected to mimic true conditions or mechanisms of injury and should be purposely selected by researchers with real life application in mind. In order to further the scope of knowledge surrounding bone fractures and healing, we selected blunt trauma injury to isolate the muscle regeneration/repair pathway and discover the cellular signaling molecules that serve in duality.

SPECIFIC AIMS

Aim 1: Characterize the process of muscle repair after blunt trauma injury by investigating the temporal expression of myogenic and myokine genes.

Aim 2: Investigate angiogenesis following muscle trauma injury by examining the temporal expression of known angiogenic genes.

METHODS

Animals

All mice used in the studies performed were approved by The Institutional Care and Use Committee at Boston University and in compliance with the Animal Welfare Act in accordance with the principles of the Guide for the Care and Use of Laboratory Animals. The mouse strain Pax7$^{tm1(cre/ER2)Gaka/J}$ (Pax7-Cre) was obtained from The Jackson Laboratories and were bred with the reporter strain, B6.Cg-Gt(ROSA)26sor<tm14(CAG-tdTomato)Hze>/J. These offspring were subsequently bred with B6,129S7-Rag1^{tm1Mom}/J mice to generate the Pax7/Ail4/Rag mice which were used in this study. Male mice were used for this study and housed in standard conditions. A total of two mice were used for each time point of the study with a total of seven time points. Male mice were used in this study.

Procedural Preparations

Tamoxifen (10 mg/ml of corn oil) (Sigma-Aldrich) was injected into the intraperitoneal space at 10 μL per gram of body weight. Two injections were administered within three days followed by a one-month wash out period.

Muscle Injury

Mice were initially anesthetized using 4% isoflurane and oxygen, and 2% to maintain condition until completion of the procedure. The total procedure ranged from 3 to 5 minutes and was performed on a warm heated mat which the mice remained on until awaking from surgery. Animals received Buprenex (analgesia) and Baytril (antibiotic prior to muscle trauma. Blunt trauma injury was introduced via a one-time

drop of a weight from a height of 31 mm to the region of the quadriceps femoris muscle (Figure 1, Figure 3). Both the right and left limbs received injury.

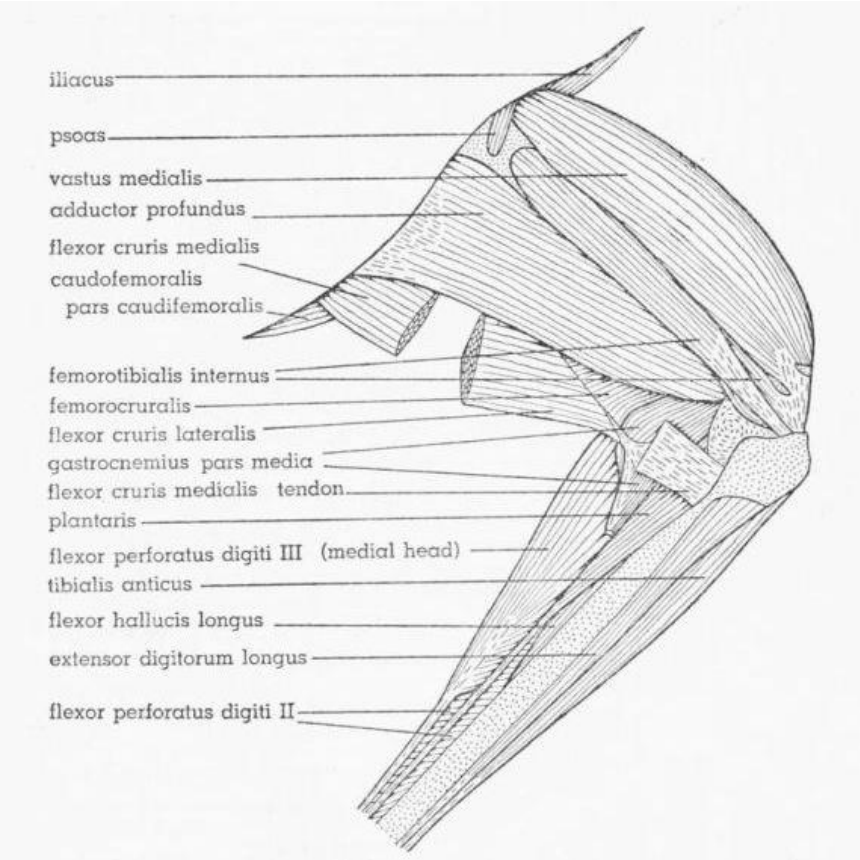

Figure 1 Muscular Anatomy of Mouse Leg This image illustrates the relative skeletal anatomy of the mouse leg. The quadriceps Femoris would drape over the visualized tissue, and was the targeted location of impact for the device pictured in **Figure 3.**

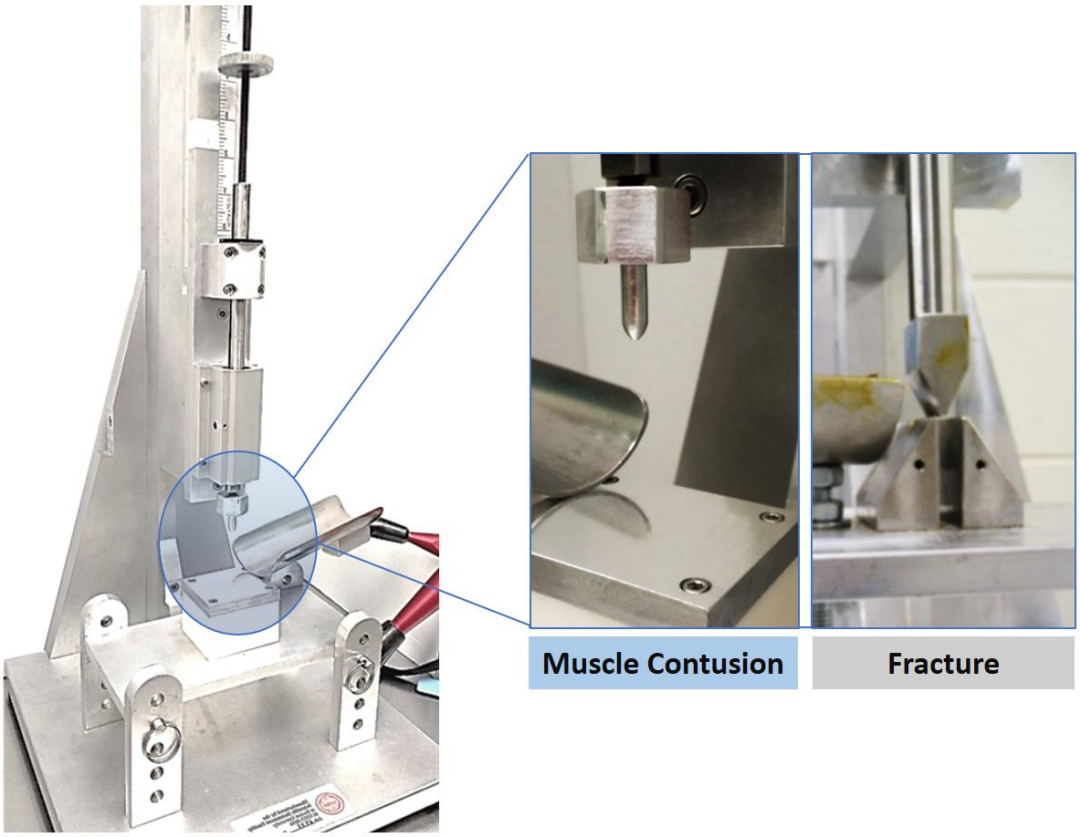

Figure 2: Muscle Contusion Device.This image illustrates the muscle contusion device used in our injury model. Mice received a single weight drop to each hind limb.

Animal Harvest

Mice were harvested at time points post-operative day (POD) 0, 2, 4, 8, 12, 16, and 24. The POD 0 animals did not receive injury and served as our controls. Animals were euthanized using carbon dioxide followed by cervical dislocation. Harvest weight was recorded. A hind limb was harvested and placed in 4% PFA for 3-4 days at 4°C. Tissue was then places in 1X PBS and stored at 4°C for future histological analysis. The remaining hind limb was used for gene expression analysis. Anterolateral femoral quadriceps muscles (including Femoris, vastus medialis) was separated from posteromedial (biceps muscles) muscle during harvest and were flash frozen in liquid nitrogen (LN_2). Samples were stored at -80 °C.

Histology and Imaging

To prepare samples for histological staining tissue was first fixed in a 4% (pH 7.4) paraformaldehyde (PFA) solution for 48-96 hours, decalcified at 4°C in Ethylenediamine Tetraacetic Acid (EDTA) for 4-5 days, and agitated in a solution of 7.5% sucrose/PBS/optimum cutting temperate (OCT) (7.5 ml) compound at 4°C overnight. Over the next two nights the agitation process was repeated with 30% sucrose/PBS/OCT and 50% sucrose/PBS/OCT respectively. Samples were embedded by immersing the sample into a basin filled with tetrafluorethane surrounded by liquid nitrogen for about one minute until the sample was completely frozen. Samples were stored in -80℃ until sectioned.

Blocks were sectioned on a Reichert-Jung Cryocut 1800 at 8-10 µm to yield 12-15 slides per tissue sample. Slides were then mounted on Superfrost Plus slides and

air dried at room temperature before storage at -20 °C. Samples used for histology were stained with hematoxylin and eosin (H&E) stains for bright field imaging or stained with Molecular Probes ProLong © Gold Antifade reagent with DAPI, (4,6-diamidino-2-phenylindole), a fluorescent stain that binds strongly to adenine–thymine rich regions in DNA. Images of tissue sections were acquired using an Olympus BX51 (Olympus America, Inc., Center Valley, PA) at 10x magnification using CellSens Dimensions 4.1.0.0, Olympus America software for photo editing.

RNA Extraction

In order to extract RNA from tissue samples, tissue was first removed from the freezer and placed on ice. 0.75 ml of Qiazol Reagent and a stainless steel ball were added to the cold sample before it was placed into the tissue lyser, Qiagen TissueLyser II. The sample was lysed for 2 or 3 intervals, or as long as it took for the sample to become liquefied but not thawed. 1 mL Qiazol and 200 µL of 1-Bromo-3-chloropropane (BCP) were then added up to 2 ml before centrifuging (Eppendorf make and model) for 15 minutes at 14000 rpm at 4 °C. The aqueous phase of the solution was transferred to a new tube with 70% ethanol and centrifuged for a total of 40 additional minutes. The extracted pellet was dissolved in RNase-free H_2O and stored at -80 °C until use.

Gel Electrophoresis, 1.5% agarose gel run at 110 V for 60-75 minutes, was used to determine the quality of extracted RNA. Absorbance spectrometry (ThermoScientific Nanodrop 2000 Spectrophotometer) was used to determine the

concentration of RNA extracted. The Nanodrop was blanked usimg ultrapure distilled water and (2μL) samples were pipetted into the reader. The absorbance was measured at settings were set to 260 and 280 nm.

Quantitative Real Time Polymerase Chain Reaction (qPCR)

RNA samples were thawed and kept on ice for the duration of this process. RNA (2μg) was diluted into 10.4 μl with RNase-free water. Reagents from Taqman Reverse Transcription Kit, RNase Inhibitor, and Taqman Reverse Transcriptase (RT) were mixed together before adding to samples. 19.6 μL of the Reverse Transcriptase Polymerase Chain Reaction (RT-PCR) was added to the 10.4 μL of RNA for a total of 30 μL. The samples were then loaded into the Eppendorf Thermal Cycler which ran at 25 °C for 10 minutes, 37 °C for 60 minutes, 95 °C for 5 minutes and finally held at 4 °C. Samples were then diluted 1:50 and stored at -20 °C.

Gene primers were purchased from Applied Biosystems and are listed in (Table 1). To prepare the samples for the RT-qPCR machine, 10 μL of Universal Master Mix (Applied Biosystems® Cat# 4304437) and 1 μL of primer set were added. A list of primers used can be found in Table 1. Each well contained 9 μL of diluted cDNA and 11 μl of the primer master mix. Each sample was run in duplicate/triplicate, with a control sample of ultrapure distilled water (9 μL) primer/master mix (11 μL) included on each plate. Samples were centrifuged for 2 minutes at 1500 rpm to get rid of bubbles, covered with clear film (Applied Biosystems Cat# 4306311) and wrapped in foil before being placed in the ABI 7700 Sequence Detector from Applied Biosystems. The RT-qPCR machine cycled 40 times

through the following cycle: 50 °C for 2 minutes, 95 °C for 15 seconds, and 60 °C for 1 minute. Threshold cycle (Ct) values were recorded. Data were analyzed using the ΔΔCt approach; target genes were normalized to 18s and control (POD 0). Results are presented as fold change compared to control.

Statistical Analysis

Statistical analysis of the data was accomplished using Microsoft Excel 2016 software. Statistical significance was determined with a single-factor ANOVA and a Tukey range test to elucidate means that were significantly different from each other. Significance value was set to $p<0.05$.

\

Primers	**Catalog Number** #4331182
18s	Mm04277571_s1
MyoD	Mm00521984_m1
Myf5	Mm00435125_m1
Myosin 1 MHC (Myh1)	Mm01332489_m1
MLC2 Myosin Light Chain – 2 (Myl2)	Mm00440384_m1
Interleukin 6 (IL-6)	Mm00446190_m1
Pax7	Mm01354484_m1
Myostatin (MSTN)	Mm01254559_m1
VegfA	Mm00437304_m1
VegfR2 (Kdr)	Mm00440099_m1
ID-1	Mm00775963_g1
Prx1	Mm00440932_m1

Table 1: Applied Biosystems Primers

RESULTS

The goals of this study are to characterize the temporal progression of myogenesis during muscle repair that will be used with future studies of muscle and bone injury. And to identify potential crosstalk mechanisms between muscle and bone repair during trauma.

Satellite/Stem Cell

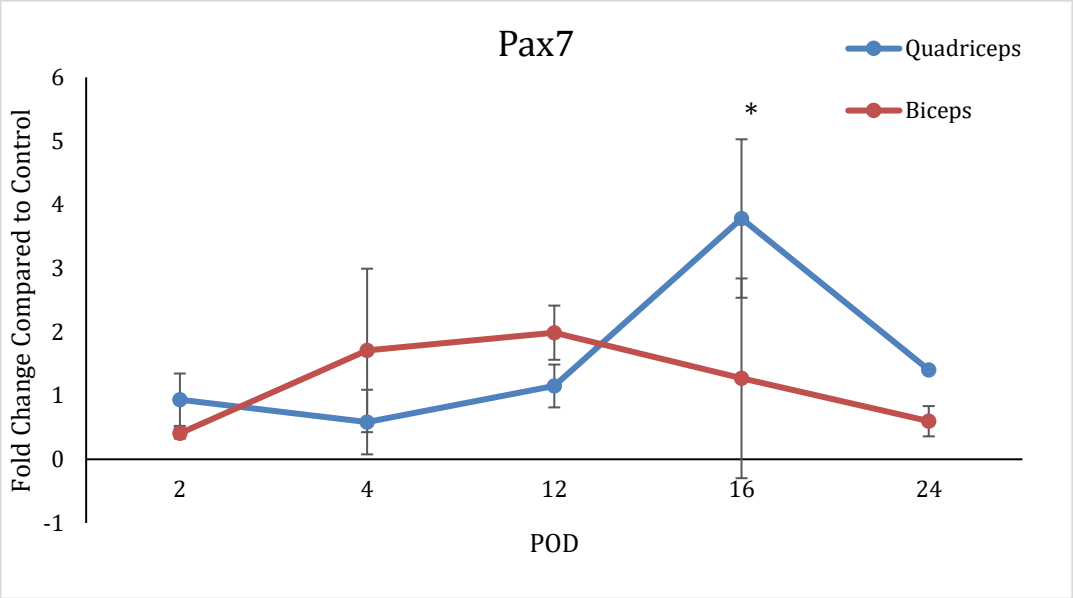

Figure 3: Pax 7 gene expression following blunt trauma injury. This figure illustrates temporal Pax 7 expression in skeletal muscle cells for 24 days. (n=2 at each time point) *denotes statistical significance at $p<0.05$.

Satellite cells are marked by the expression of Pax 7. Femoral quadriceps muscles show an initial decrease in Pax 7 expression at POD 4 (Figrure 4). The expression of Pax 7 in the quadriceps reaches a peak, approximately a 4 fold increase compared to the control muscle at POD 16. The expression returns to baseline by POD

24. The difference in means at POD 4 and POD 16 proved to be statistically significant with $p<0.05$. While in the biceps muscles the expression of Pax 7 shows a non-significant increase from POD 2 to POD 12.

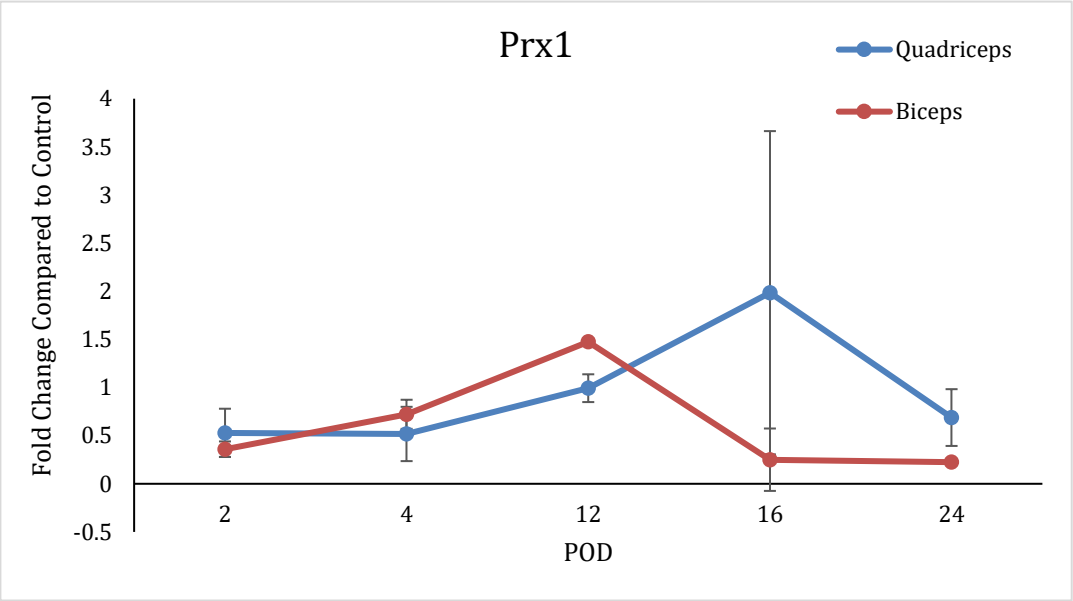

Figure 4: Prx1 gene expression following blunt trauma injury. This figure illustrates temporal Prx1 expression in skeletal muscle cells for 24 days. (n=2 at each time point)

The Prx1 expression cell population is known to contribute to fracture repair and ectopic bone formation. The expression of Prx1 in the femoral quadriceps muscles show a peak expression of approximately 2 fold over the control at POD 16. The expression returns to baseline by POD 24. While in the biceps muscles the expression of Pax 7 show a 1.5-fold increase compared to the control muscle at POD 12.

Myogenic Genes

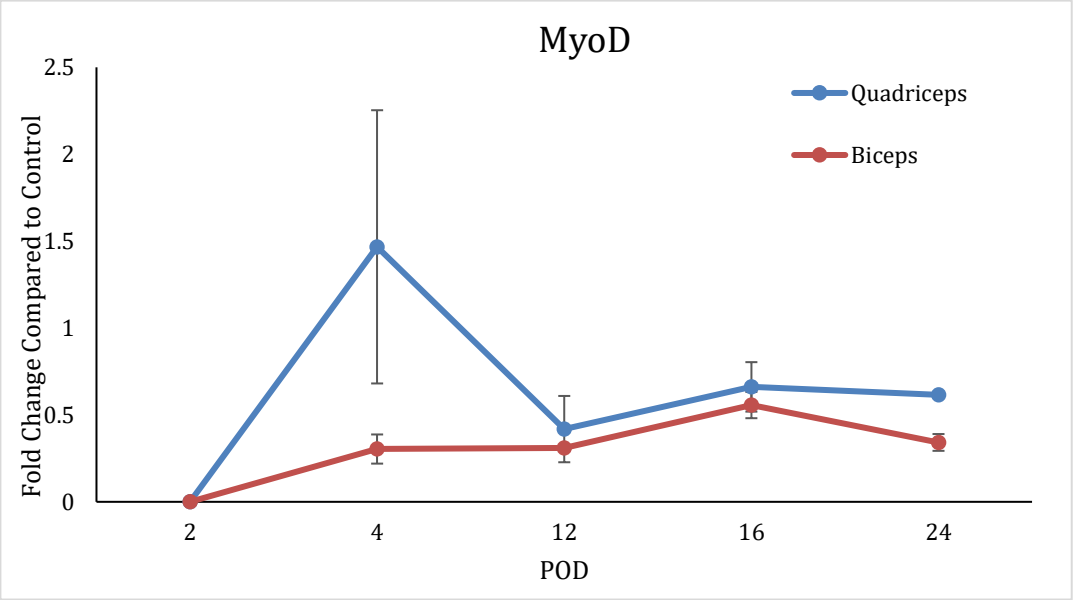

Figure 5: MyoD gene expression following blunt trauma injury. This figure illustrates Myf5 expression in skeletal muscle cells for 24 days following blunt trauma injury. (n=2 at each time point) $p<0.05$

During myogenesis, the expression of MyoD increases indicating cell lineage commitment and myogenic programming is marked by increased Myf5 protein. In this model of muscle regeneration, MyoD gene expression in the femoral quadriceps and biceps muscles were undetectable on POD 2 (Figure 6). In the femoral biceps muscles, the expression of MyoD increased to a quarter of the baseline expression at POD 4. Between POD 12 and 16 the MyoD expression increased to nearly half of the baseline gene expression. And by POD 24 the MyoD gene expression returned to near its POD 4 expression levels. MyoD detected in the femoral quadriceps muscles at POD 4 was shown to be 1.5 times that of control levels before decreasing to half of the expression levels of the control at POD 12 through POD 24.

In the femoral quadriceps muscles Myf 5 expression was near baseline at POD 2 and increased to 1.75 times the control expression at POD 4 (Figure 7). The Myf 5

expression decreased at POD 12, however, the expression rebounded to approximately 1.5 times the control expression at POD 24. The expression of Myf5 in the femoral biceps muscles did not show change in expression across time.

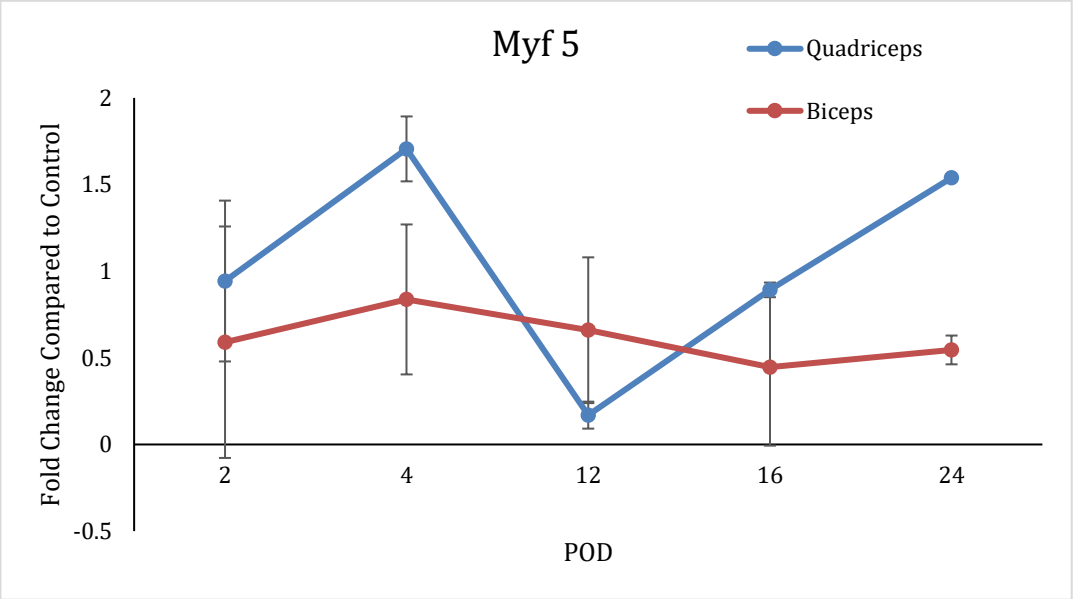

Figure 6: Myf5 gene expression following blunt trauma injury. This figure illustrates temporal Myf 5 expression in skeletal muscle cells for 24 days following blunt trauma injury. (n=2 at each time point) $p<0.05$.

The adult myosin light chain and adult myosin heavy chain are expressed in myofibers. These genes were probed in this muscle injury model (Figure 8 and 9). In the biceps, Myl2 (myosin light chain 2), expression was at baseline at POD 2, however, by POD 4 the gene expression showed approximately a 6-fold increase over the control muscle. Between POD 4 and POD 12 the expression levels of Myl2 decreased to near baseline and continued to decrease through POD 16 and 24. At POD 24 expression was close to undetectable. Myl2 expression in the quadriceps showed very little fluctuation between POD 2 through POD 12, with expression levels

remaining near baseline. At POD 16 Myl2 expression increased to 3-fold compared to the control and by POD 24 the expression levels were 17-fold compared to control.

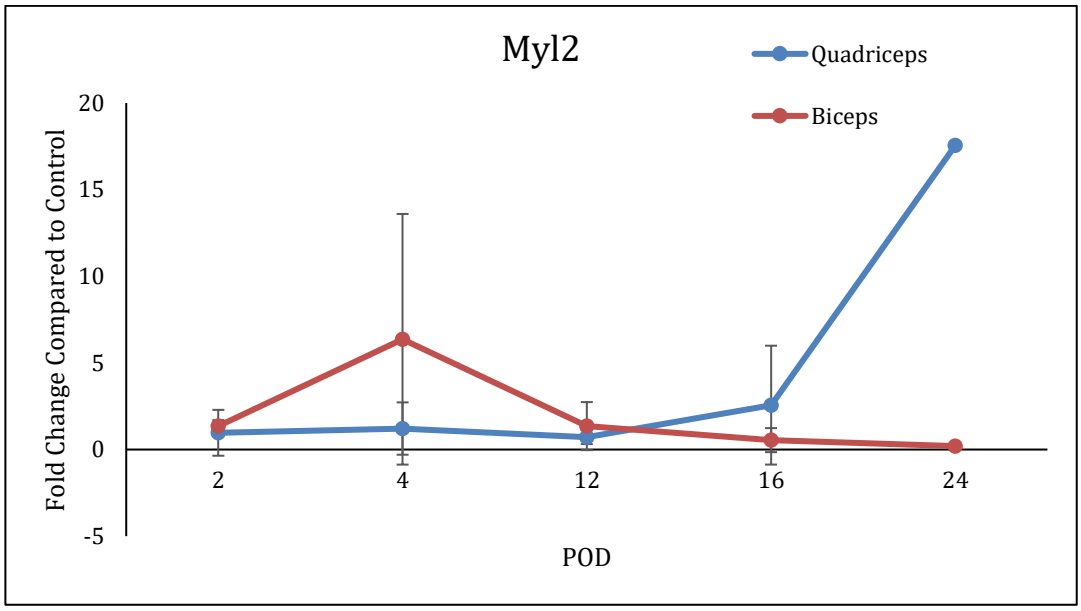

Figure 7: Myl2 gene expression following blunt trauma injury. This figure illustrates Myl2 expression in skeletal muscle cells for 24 days following blunt trauma injury. (n=2 at each time point) **p<0.05.**

Similar levels of myosin heavy chain (Myh1) expression were detected between the femoral biceps muscles and the femoral quadriceps muscles at POD 2 through POD 12. POD 16 there was a divergence of expression levels with Myh1 levels in the femoral bicep muscles decreasing to less than a fifth of the control values at POD 16 and a tenth of the control expression at POD 24. In the quadriceps Myh1 expression increased from baseline at POD 12 to a 2-fold change compared to the control at POD 16. Myh1 expression at POD 24 was undetectable.

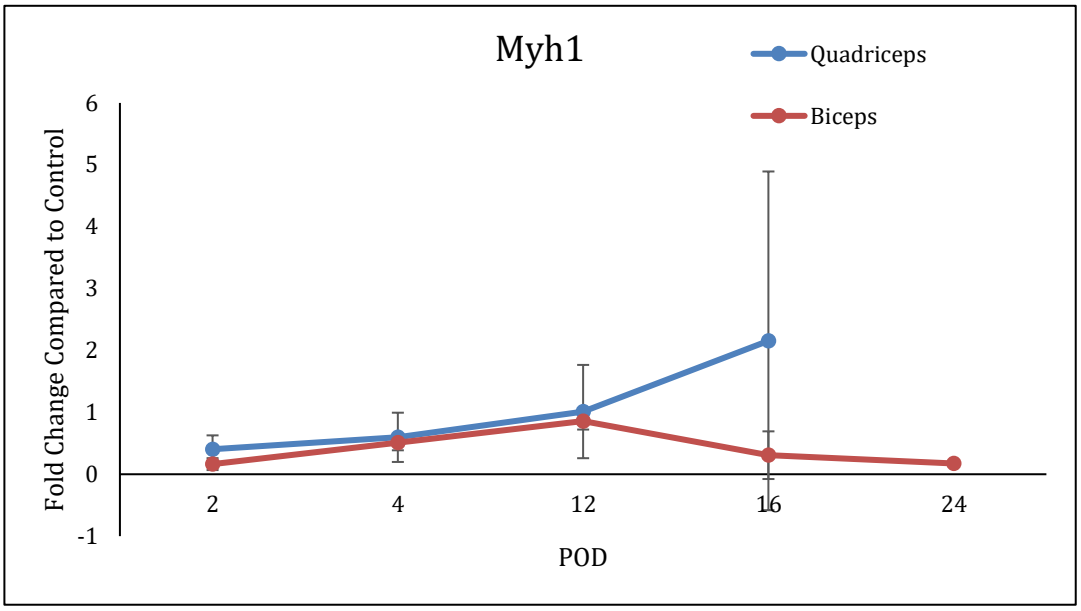

Figure 8: Myh1 gene expression following blunt trauma injury. This figure illustrates Myh1 expression in skeletal muscle cells for 24 days following blunt trauma injury. (n=2 at each time point) $p<0.05$.

Angiogenesis

VEGF-A expression in the femoral biceps muscles at POD 2 was 1.25 fold above control values, and decreased to half of the baseline expression by POD 4 (Figure 10). And showed a non-significant peak at POD 12. In the femoral quadriceps muscles VEGF-A expression was half of the expression of the control values at POD 2 and showed a slight decreased at POD 4. The expression of VEGF-A showed a steady increase in expression through POD 16 with a 1.5 fold change compared to the control muscle. However, at POD 24, VEGF-A levels in the femoral quadriceps muscles decreased to around three-quarters of the baseline expression in the muscle.

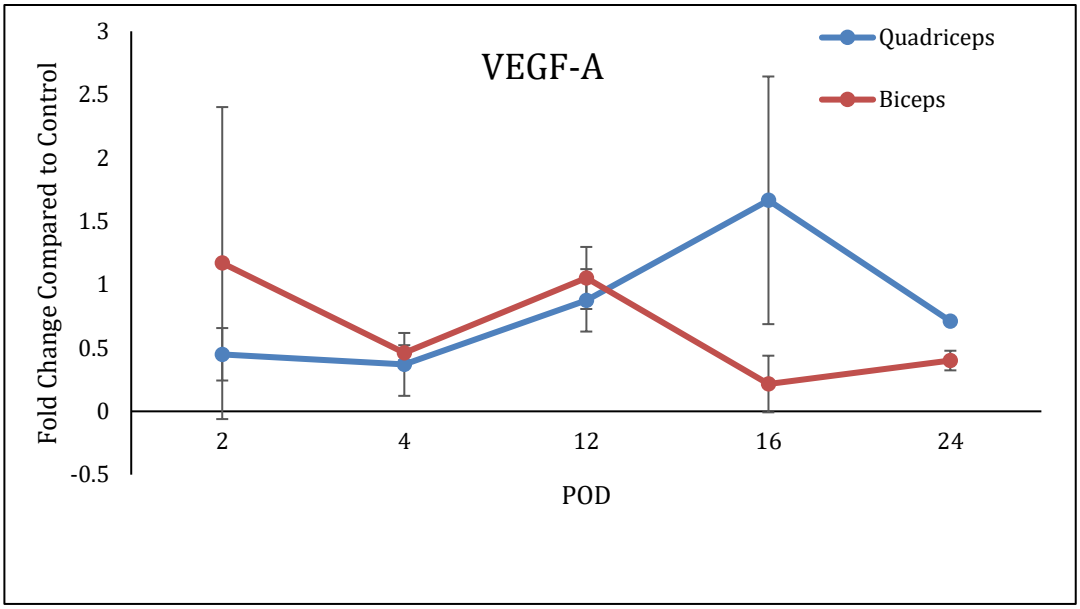

Figure 9: VEGF-A gene expression following blunt trauma injury. This graph illustrates VEGF-A gene expression in skeletal muscle for 24 days following blunt trauma injury. (n=2 at each time point) $p<0.05$

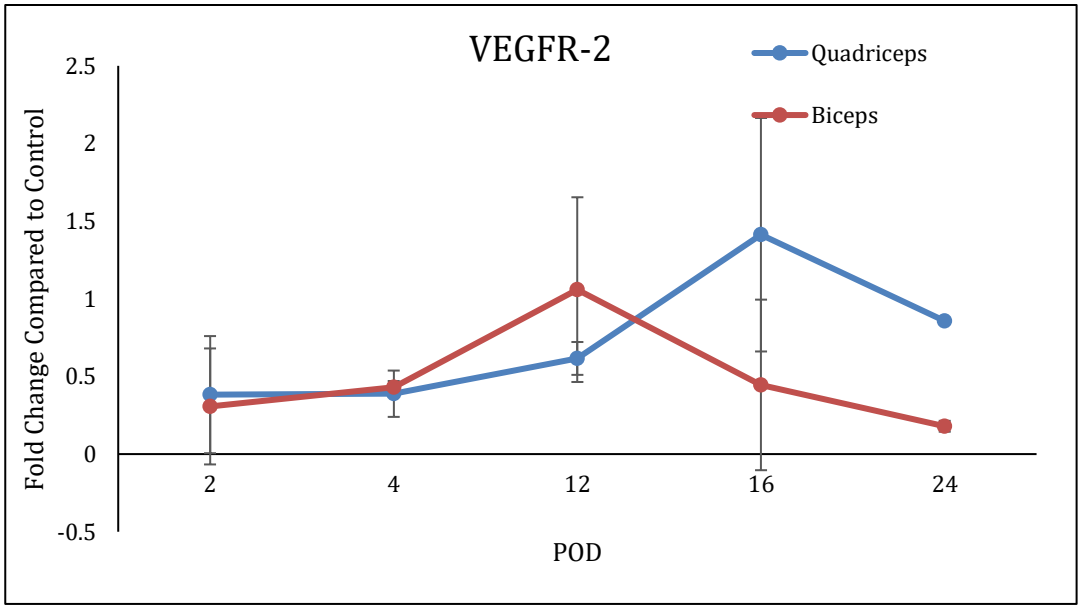

Figure 10: VEGF-A gene expression following blunt trauma injury. This graph illustrates VEGFR2 gene expression in skeletal muscle for 24 days following blunt trauma injury. (n=2 at each time point) $p<0.05$

In the femoral biceps muscles the VEGFR-2 expression was a quarter of the control expression values at POD 2 (Figure 11). The peak expression of VEGFR-2 was at POD 12 and was about the same as to the control values. The expression decreased at POD 16 and continued to show low levels of expression through POD 24. VEGFR-2 gene expression in the femoral quadriceps muscles remained fairly constant from POD 2 through POD 4, remaining at forty-percent of the control baseline. At peak expression there was a 1.5-fold change compared to control values at POD 16.

Myokines

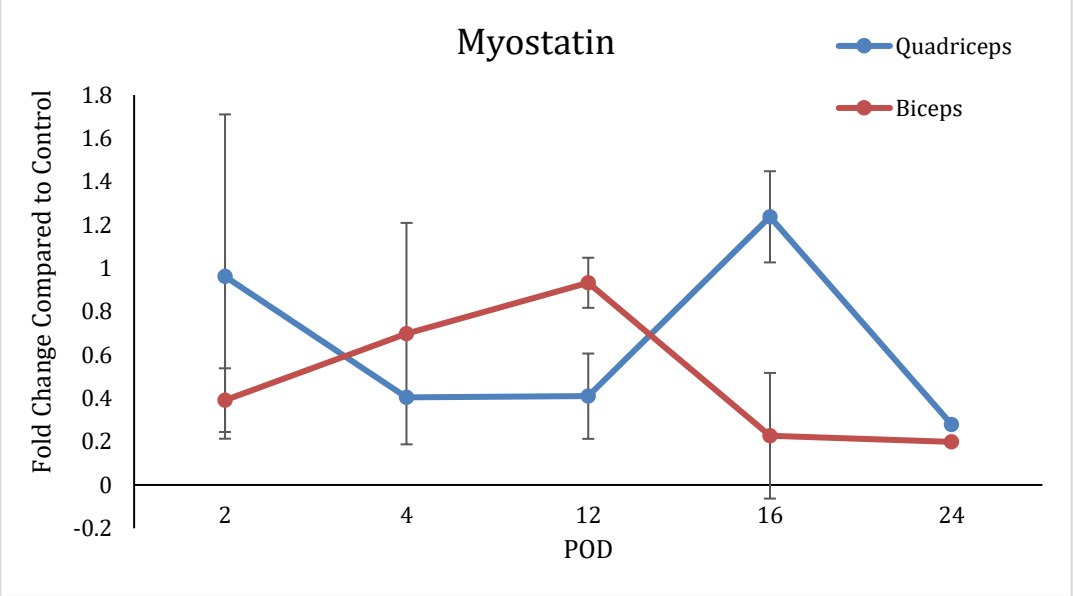

Figure 11: Myostatin gene expression following blunt trauma injury. This graph illustrates myostatin gene expression in skeletal muscle for 24 days following blunt muscle trauma. (n=2 at each time point)

Myostatin is a myokine and is a negative regulator of muscle mass. The expression of Myostatin in the femoral biceps muscles at POD 2 showed about a 0.4

fold change compared to the control and increased through POD 12 when expression peaked (Figure 12). Myostatin expression in the femoral quadriceps muscles showed not changed compared to the control at POD 2 but decreased with a 0.4 fold change at POD 4. By POD 16, Myostatin expression peaked with a 1.2-fold change.

Interleukin-6 expression is also known as a myokine. The expression of IL-6 in the femoral biceps muscles showed a 0.5 fold change compared to the control muscles at POD 2 (Figure 13). The expression increased 1.5 fold at POD 4 which was the peak expression. In the quadriceps IL-6 expression showed a 1.5 fold increase compared to the control muscle at POD 2. The expression continued to increase at POD 4 but decreased to baseline levels at POD 12. Expression increased to nearly 2.5-fold control values at POD 16.

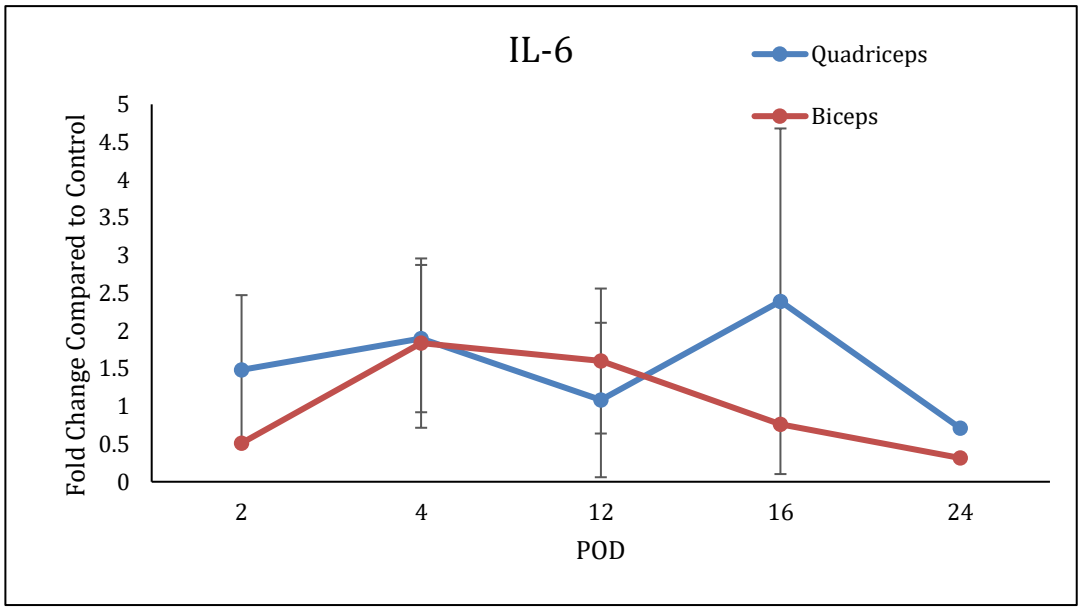

Figure 12: IL-6 gene expression following blunt trauma injury. This figure illustrates IL-6 gene expression in skeletal muscle cells for 24 days following blunt trauma injury. (n=2 at each time point) $p<0.05$

BMP Signaling

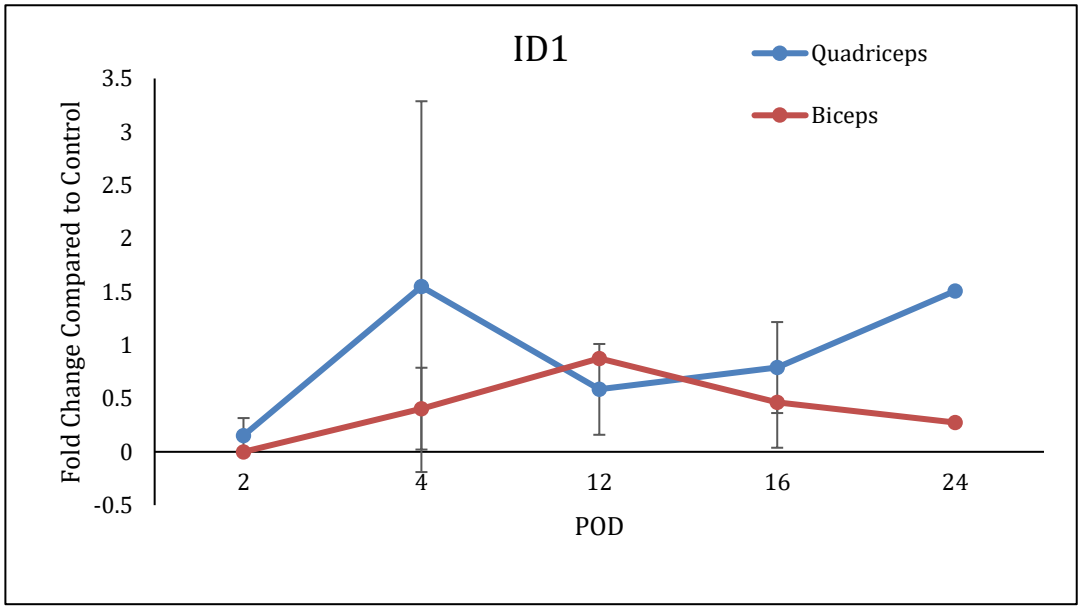

Figure 13: ID1 gene expression following blunt trauma injury. This figure illustrates ID1 gene expression in skeletal muscle cells for 24 days following blunt trauma injury. (n=2 at each time point) $p<0.05$

BMP signaling induces the expression of ID1. There was little expression of ID1 in the femoral biceps muscles at POD 2 (Figure 15). The gene expression increased to about half of the control muscle values at POD 4 and approached baseline levels by POD 12. The expression of ID1 peaked at POD 12 followed by a decrease to half of control expression values at POD 16. ID1 expression in the femoral quadriceps muscles at POD 2 was around one-fifth of control values. By POD 4, ID1 expression was 1.5 times the expressive values of the control muscle. Between POD 4 and POD 12 the expression decreased to half of the control muscle values before increasing to baseline by POD 16 and at POD 24 increased approximately 1.5-fold compared to control muscle.

DISCUSSION

We've learned from Hardy et al. that damaged skeletal muscle repairs at a variable pace depending on the type of injury. Most skeletal muscle studies set a repair period of one-month after onset of injury, and some choose to extend the observation period up to three months. Here we look at 24 days to suggest a trend in the overall healing process of skeletal muscle due to blunt force trauma. Muscle impacted by the muscle contusion device exists in the area of the quadriceps, while muscle not in the direct path of the device would likely be found in the biceps.

Pax 7 expression

Pax 7 expression in actively proliferating satellite cells is lowered compared to quiescent cells and down regulated in cells committed to terminal differentiation (Olguin et al., 2007). We've also seen that satellite cells are activated as early as 18 hours post trauma due to chemical stimulus (Baoge et al., 2012) one would expect a lowered Pax 7 expression in these proliferating cells. The quadriceps being in direct line of injury show a dip in gene expression compared to the control four days after injury.

Ectopic expression of Pax7 can efficiently repress the MyoD-dependent conversion of mesenchymal cells to the muscle lineage. Overexpression of Pax-7 also promotes cell cycle exit even in proliferation conditions. Together, these results

suggest that Pax-7 may play a crucial role in allowing activated satellite cells to reacquire a quiescent, undifferentiated state.

Myogenic gene expression

MyoD plays a major role in inducing cells into the myogenic lineage but has very little expression in mature skeletal muscle cells. Fig. 6 shows MyoD had undetectable values two post injury and spike in expression by day four. This could suggest that MyoD aided in the induction of satellite cell proliferation into the myogenic lineage. Seeing the spike only in the quadriceps muscle and not the biceps muscle may also suggest that because the quadriceps cells dealt with the brunt force of the trauma, the damage induced the MyoD only on the lateral side of the skeletal muscle.

Myf5 functions in myogenesis as a cell cycle regulator, as Myf 5 expression regulates when cells will enter or exit the cell cycle. Myf 5 expression should increase as a skeletal muscle matures, with its highest expression occurring in adult skeletal muscle because adult muscle has exited the cell cycle. Fig. 5 shows a fairly stable level of Myf 5 expression in the bicep muscle, which was deep to the muscle contusion injury. The expression of Myf 5 after day twelve of injury may suggest that there is an increase in the number of maturing skeletal muscle fibers, or an increase in Myf 5 signaling to nearby skeletal muscle.

Myosin light chain kinase and myosin heavy chain are both components of adult skeletal muscle. Expression of both contractile proteins should increase as healing

continues to occur in days post injury. In Fig. 7 we see that the expression of myosin light chain kinase does not increase in the quadriceps muscle until after the twelfth day post injury. The spike in seen after day sixteen may suggest that the skeletal muscle has left the repair phase of healing and enters the remodeling phase. The repair phase is characterized by the regeneration of myofibers and the formation of scar tissue and the remodeling phase is defined by the maturation of myoblasts into myofibers and the reorganization of the muscle through contractions, which requires light chain kinase. Myosin heavy chain kinase shows a similar trend to the activity of myosin light chain kinase. After day twelve there is marked increase in the expression of the ATP-dependent heavy chain myosin which showed an upward trend though from days twelve to sixteen.

Angiogenic gene expression

Interleukin-1 is a powerful inflammatory cytokine that aid in maturing neutrophils for their role in removing necrotic tissue after damage has occurred. Fig. 9 shows that four days after injury IL-1 levels remained 1.5 fold over their control counterparts. This is in accordance with the fact that neutrophil levels can remain elevated for up to five fays with skeletal muscle injury (Tidball et al., 2005). Seeing the change in expression occur first in the quadriceps and then a smaller increase in IL-1 in the biceps on day twelve may suggest that a directional or wave movement of the immune response through damaged tissues.

By examining IL-6 expression we would not expect to see excess production of IL-6, as it may indicate improper muscle healing and or functioning. IL-6 levels can

also assess the overall health of the muscle days after injury. Fig. 10 shows an initially higher IL-6 level in day two POD muscle why may suggest that IL-6 infiltration to the site of damage in the quadriceps. On day four we see that the level of IL-6 has equated between the bicep and the quadriceps which reiterates the findings of Tidball et al. Compared to the IL-6 levels in the biceps, which peak on day four and decline over the next twenty days, the spike on day 16 of IL-6 in the quadriceps muscle may be an indication secondary injury, or delayed healing.

VEGF-A is a proangiogenic growth factor that exists in endothelial cell-cell junctions. VEGF-A also induces mitosis in endothelial cells. Fig. 11 shows an increase in VEGF-A expression in the quadriceps with a peak at POD sixteen, which may suggest the surrounding demand for an expanded microvasculature. VEGF-A expression also increases when there is stretch tension on capillary walls or hyperemia, due to increased blood flow through the vasculature. The drop in expression of VEGF-A in the quadriceps after day sixteen may indicate that the vascular regeneration process is completed in majority by that time.

VEGFR-2 is part of a complex that transduces signals related to the turbulence of blood flow to polarity molecules that alter gene expression. Fig. 12 shows an increase of the expression of VEGFR-2 from POD day 2 until POD day 16, and then a drop in the quadriceps expression. Conversely the POD day 2 value of the bicep VEGFR-2 may suggest that the bicep muscles experienced an increase in turbulent blood flow between the initial injury and POD 2. As the quadriceps regenerated skeletal muscle fibers and vasculature, turbulent or increased blood flow in the bicep

capillaries may be reflected as the near parallel increase in VEGF-A among both muscle groups.

Myostatin (MSTN) is a muscle derived protein of the TGF-β family, with an inhibitory role in muscle growth and fracture repair. MSTN expression is elevated with significant musculoskeletal injury, though this remains poorly understood. Fig. 13 shows peaks in MSTN in the bicep on day twelve and on the quadriceps on day sixteen. This may suggest a regulatory mechanism that helps prevent unnecessary hypertrophy in skeletal muscle tissue after weeks of regeneration.

Conclusion and Future Directions

Overall this study hoped to elucidate some of the highly coordinated processes of skeletal muscle repair and regeneration. There are many complex mechanisms involved in the muscle repair and regeneration pathway that are yet to be understood. In further studies, researchers should aim to expand their sample size to $N \geq 5$ per time point in order to better reflect behavioral population. We would also recommend smaller dilutions (1:5 or no dilution) of the cDNA used to run the primers in RT-qPCR in order to reduce the chance of getting more undetectable values in the RT-qPCR results.

REFERENCES

Armand, A.-S., Launay, T., Pariset, C., Della Gaspera, B., Charbonnier, F., & Chanoine, C. (2003). Injection of FGF6 accelerates regeneration of the soleus muscle in adult mice. *Biochimica et Biophysica Acta (BBA) - Molecular Cell Research*, *1642*(1), 97–105. https://doi.org/10.1016/S0167-4889(03)00103-4

Baoge, L., Van Den Steen, E., Rimbaut, S., Philips, N., Witvrouw, E., Almqvist, K. F., … Vanden Bossche, L. C. (2012). Treatment of Skeletal Muscle Injury: A Review [Research article]. https://doi.org/10.5402/2012/689012

Beebe, F. A., Barkin, R. L., & Barkin, S. (2005). A clinical and pharmacologic review of skeletal muscle relaxants for musculoskeletal conditions. *American Journal of Therapeutics*, *12*(2), 151–171.

Buckingham, M. (2017). Gene regulatory networks and cell lineages that underlie the formation of skeletal muscle. *Proceedings of the National Academy of Sciences of the United States of America*, *114*(23), 5830–5837. https://doi.org/10.1073/pnas.1610605114

Chan, Y.-S., Li, Y., Foster, W., Fu, F. H., & Huard, J. (2005). The Use of Suramin, an Antifibrotic Agent, to Improve Muscle Recovery after Strain Injury. *The American Journal of Sports Medicine*, *33*(1), 43–51. https://doi.org/10.1177/0363546504265190

Christov, C., Chrétien, F., Abou-Khalil, R., Bassez, G., Vallet, G., Authier, F.-J., … Gherardi, R. K. (2007). Muscle Satellite Cells and Endothelial Cells: Close Neighbors and Privileged Partners. *Molecular Biology of the Cell*, *18*(4), 1397–1409. https://doi.org/10.1091/mbc.E06-08-0693

Conway, D. E., Coon, B. G., Budatha, M., Arsenovic, P. T., Orsenigo, F., Wessel, F., … Schwartz, M. A. (2017). VE-cadherin phosphorylation regulates endothelial fluid shear stress responses through the polarity protein LGN. *Current Biology : CB*, *27*(14), 2219-2225.e5. https://doi.org/10.1016/j.cub.2017.06.020

Davis, K. M., Griffin, K. S., Chu, T.-M. G., Wenke, J. C., Corona, B. T., McKinley, T. O., & Kacena, M. A. (2015). Muscle-bone interactions during fracture healing. *Journal of Musculoskeletal & Neuronal Interactions*, *15*(1), 1–9.

Dinarello, C. A., Simon, A., & van der Meer, J. W. M. (2012). Treating inflammation by blocking interleukin-1 in a broad spectrum of diseases. *Nature Reviews. Drug Discovery*, *11*(8), 633–652. https://doi.org/10.1038/nrd3800

Dunn, A., Talovic, M., Patel, K., Patel, A., Marcinczyk, M., & Garg, K. (n.d.). Biomaterial and stem cell-based strategies for skeletal muscle regeneration. *Journal of Orthopaedic Research*, *0*(0). https://doi.org/10.1002/jor.24212

Einhorn, T. A., & Gerstenfeld, L. C. (2015). Fracture healing: mechanisms and interventions. *Nature Reviews. Rheumatology*, *11*(1), 45–54. https://doi.org/10.1038/nrrheum.2014.164

Forcina, L., Miano, C., & Musarò, A. (2018). The physiopathologic interplay between stem cells and tissue niche in muscle regeneration and the role of IL-6 on muscle homeostasis and diseases. *Cytokine & Growth Factor Reviews*, *41*, 1–9. https://doi.org/10.1016/j.cytogfr.2018.05.001

Fukushima, K., Badlani, N., Usas, A., Riano, F., Fu, F. H., & Huard, J. (2001). The Use of an Antifibrosis Agent to Improve Muscle Recovery after Laceration. *The American*

Journal of Sports Medicine, *29*(4), 394–402. https://doi.org/10.1177/03635465010290040201

Gao, X., Usas, A., Tang, Y., Lu, A., Tan, J., Schneppendahl, J., … Huard, J. (2014). A comparison of bone regeneration with human mesenchymal stem cells and muscle derived stem cells and the critical role of BMP. *Biomaterials*, *35*(25), 6859–6870. https://doi.org/10.1016/j.biomaterials.2014.04.113

Gerstenfeld, L. C., Alkhiary, Y. M., Krall, E. A., Nicholls, F. H., Stapleton, S. N., Fitch, J. L., … Einhorn, T. A. (2006). Three-dimensional Reconstruction of Fracture Callus Morphogenesis. *Journal of Histochemistry & Cytochemistry*, *54*(11), 1215–1228. https://doi.org/10.1369/jhc.6A6959.2006

Goel, A. J., Rieder, M.-K., Arnold, H.-H., Radice, G. L., & Krauss, R. S. (2017). Niche Cadherins Control the Quiescence-to-Activation Transition in Muscle Stem Cells. *Cell Reports*, *21*(8), 2236–2250. https://doi.org/10.1016/j.celrep.2017.10.102

Hacking, C. (No Date). Gustilo Anderson classification | Radiology Reference Article | Radiopaedia.org. Retrieved March 31, 2019, from https://radiopaedia.org/articles/gustilo-anderson-classification

Hardy, D., Besnard, A., Latil, M., Jouvion, G., Briand, D., Thépenier, C., … Chrétien, F. (2016). Comparative Study of Injury Models for Studying Muscle Regeneration in Mice. *PLoS ONE*, *11*(1). https://doi.org/10.1371/journal.pone.0147198

Hill, M. (2019, January 21). Musculoskeletal System Development - Embryology. Retrieved March 27, 2019, from

https://embryology.med.unsw.edu.au/embryology/index.php/Musculoskeletal_System_Development

Huard, J., Li, Y., & Fu, F. H. (2002). Muscle Injuries and Repair: Current Trends in Research. *JBJS*, *84*(5), 822.

Hurtgen, B. J., Ward, C. L., Garg, K., Pollot, B. E., Goldman, S. M., McKinley, T. O., … Corona, B. T. (n.d.). Severe muscle trauma triggers heightened and prolonged local musculoskeletal inflammation and impairs adjacent tibia fracture healing, 13.

Hurtgen et al. - Severe muscle trauma triggers heightened and prolo.pdf. (n.d.). Retrieved from http://www.ismni.org/jmni/pdf/64/jmni_16_122.pdf

Index of /sites/gutenberg.org/4/1/8/1/41812/41812-h/images. (n.d.). Retrieved March 30, 2019, from http://mirrorservice.org/sites/gutenberg.org/4/1/8/1/41812/41812-h/images/

Järvinen, T. A. H., Järvinen, T. L. N., Kääriäinen, M., Kalimo, H., & Järvinen, M. (2005). Muscle Injuries: Biology and Treatment. *The American Journal of Sports Medicine*, *33*(5), 745–764. https://doi.org/10.1177/0363546505274714

Kansal, R., Kanojia, R. K., Kumar, V., Vaiphei, K., & Dhillon, M. S. (2019). Role of PAX-7 as a tissue marker in mangled extremity: a pilot study. *European Journal of Orthopaedic Surgery & Traumatology*. https://doi.org/10.1007/s00590-019-02410-w

Kasemkijwattana. (n.d.). Use of Growth Factors to Improve Muscle Healing After Strain Injury. *Clinical Orthopaedics and Related Research.*, *370*, 272–285.

Kasemkijwattana, C., Menetrey, J., Somogyi, G., Moreland, M. S., Fu, F. H., Buranapanitkit, B., … Huard, J. (1998). Development of approaches to improve the

healing following muscle contusion. *Cell Transplantation*, *7*(6), 585–598. https://doi.org/10.1016/S0963-6897(98)00037-2

Kitzmann, M., Carnac, G., Vandromme, M., Primig, M., Lamb, N. J. C., & Fernandez, A. (1998). The Muscle Regulatory Factors MyoD and Myf-5 Undergo Distinct Cell Cycle–specific Expression in Muscle Cells. *The Journal of Cell Biology*, *142*(6), 1447–1459.

Latroche, C., Weiss-Gayet, M., Muller, L., Gitiaux, C., Leblanc, P., Liot, S., … Chazaud, B. (2017). Coupling between Myogenesis and Angiogenesis during Skeletal Muscle Regeneration Is Stimulated by Restorative Macrophages. *Stem Cell Reports*, *9*(6), 2018–2033. https://doi.org/10.1016/j.stemcr.2017.10.027

Lepper, C., & Fan, C.-M. (2012). Generating Tamoxifen-Inducible Cre Alleles to Investigate Myogenesis in Mice. *Methods in Molecular Biology (Clifton, N.J.)*, *798*, 297–308. https://doi.org/10.1007/978-1-61779-343-1_17

Maes, C., Kobayashi, T., & Kronenberg, H. M. (2007). A Novel Transgenic Mouse Model to Study the Osteoblast Lineage in Vivo. *Annals of the New York Academy of Sciences*, *1116*(1), 149–164. https://doi.org/10.1196/annals.1402.060

Marsell, R., & Einhorn, T. A. (2011). THE BIOLOGY OF FRACTURE HEALING. *Injury*, *42*(6), 551–555. https://doi.org/10.1016/j.injury.2011.03.031

Miller, K. J., Thaloor, D., Matteson, S., & Pavlath, G. K. (2000). Hepatocyte growth factor affects satellite cell activation and differentiation in regenerating skeletal muscle. *American Journal of Physiology-Cell Physiology*, *278*(1), C174–C181. https://doi.org/10.1152/ajpcell.2000.278.1.C174

Neill, T., Schaefer, L., & Iozzo, R. V. (2012). Decorin. *The American Journal of Pathology*, *181*(2), 380–387. https://doi.org/10.1016/j.ajpath.2012.04.029

Nozaki, M., Li, Y., Zhu, J., Ambrosio, F., Uehara, K., Fu, F. H., & Huard, J. (2008). Improved Muscle Healing after Contusion Injury by the Inhibitory Effect of Suramin on Myostatin, a Negative Regulator of Muscle Growth. *The American Journal of Sports Medicine*, *36*(12), 2354–2362. https://doi.org/10.1177/0363546508322886

Olfert, I. M., Baum, O., Hellsten, Y., & Egginton, S. (2016). Advances and challenges in skeletal muscle angiogenesis. *American Journal of Physiology - Heart and Circulatory Physiology*, *310*(3), H326–H336. https://doi.org/10.1152/ajpheart.00635.2015

Olguin, H. C., Yang, Z., Tapscott, S. J., & Olwin, B. B. (2007). Reciprocal inhibition between Pax7 and muscle regulatory factors modulates myogenic cell fate determination. *The Journal of Cell Biology*, *177*(5), 769–779. https://doi.org/10.1083/jcb.200608122

Relaix et al. - 2006 - Pax3 and Pax7 have distinct and overlapping functi.pdf. (n.d.). Retrieved from http://jcb.rupress.org/content/jcb/172/1/91.full.pdf

Relaix, F., Montarras, D., Zaffran, S., Gayraud-Morel, B., Rocancourt, D., Tajbakhsh, S., … Buckingham, M. (2006). Pax3 and Pax7 have distinct and overlapping functions in adult muscle progenitor cells. *The Journal of Cell Biology*, *172*(1), 91–102. https://doi.org/10.1083/jcb.200508044

Rogers, M. B., Shah, T. A., & Shaikh, N. N. (2015). Turning Bone Morphogenetic Protein 2 (BMP2) On and Off in Mesenchymal Cells. *Journal of Cellular Biochemistry*, *116*(10), 2127–2138. https://doi.org/10.1002/jcb.25164

Shah, K., Majeed, Z., Jonason, J., & O'Keefe, R. J. (2013). The Role of Muscle in Bone Repair: the Cells, Signals, and Tissue Responses to Injury. *Current Osteoporosis Reports*, *11*(2), 130–135. https://doi.org/10.1007/s11914-013-0146-3

Sheikh, F., Lyon, R. C., & Chen, J. (2015). Functions of myosin light chain-2 (MYL2) in cardiac muscle and disease. *Gene*, *569*(1), 14–20. https://doi.org/10.1016/j.gene.2015.06.027

Singh, D. P., Barani Lonbani, Z., Woodruff, M. A., Parker, T. J., Steck, R., & Peake, J. M. (2017). Effects of Topical Icing on Inflammation, Angiogenesis, Revascularization, and Myofiber Regeneration in Skeletal Muscle Following Contusion Injury. *Frontiers in Physiology*, *8*. https://doi.org/10.3389/fphys.2017.00093

Stantzou, A., Schirwis, E., Swist, S., Alonso-Martin, S., Polydorou, I., Zarrouki, F., … Amthor, H. (2017). BMP signaling regulates satellite cell-dependent postnatal muscle growth. *Development (Cambridge, England)*, *144*(15), 2737–2747. https://doi.org/10.1242/dev.144089

Sternberg, N., & Hamilton, D. (1981). Bacteriophage P1 site-specific recombination: I. Recombination between loxP sites. *Journal of Molecular Biology*, *150*(4), 467–486. https://doi.org/10.1016/0022-2836(81)90375-2

Takahashi, T., Ishida, K., Itoh, K., Konishi, Y., Yagyu, K.-I., Tominaga, A., … Yamamoto, H. (2003). IGF-I gene transfer by electroporation promotes regeneration in a muscle injury model. *Gene Therapy*, *10*(8), 612–620. https://doi.org/10.1038/sj.gt.3301900

Tichy, E. D., Sidibe, D. K., Greer, C. D., Oyster, N. M., Rompolas, P., Rosenthal, N. A., … Mourkioti, F. (2018). A robust Pax7EGFP mouse that enables the visualization of dynamic behaviors of muscle stem cells. *Skeletal Muscle*, *8*. https://doi.org/10.1186/s13395-018-0169-7

Tidball, J. G. (2005). Inflammatory processes in muscle injury and repair. *American Journal of Physiology-Regulatory, Integrative and Comparative Physiology*, *288*(2), R345–R353. https://doi.org/10.1152/ajpregu.00454.2004

Uchida, C., Nwadozi, E., Hasanee, A., Olenich, S., Olfert, I. M., & Haas, T. L. (2015). Muscle-derived vascular endothelial growth factor regulates microvascular remodelling in response to increased shear stress in mice. *Acta Physiologica (Oxford, England)*, *214*(3), 349–360. https://doi.org/10.1111/apha.12463

Wilk, K., Yeh, S.-C. A., Mortensen, L. J., Ghaffarigarakani, S., Lombardo, C. M., Bassir, S. H., … Intini, G. (2017). Postnatal Calvarial Skeletal Stem Cells Expressing PRX1 Reside Exclusively in the Calvarial Sutures and Are Required for Bone Regeneration. *Stem Cell Reports*, *8*(4), 933–946. https://doi.org/10.1016/j.stemcr.2017.03.002

Xu, P., Werner, J.-U., Milerski, S., Hamp, C. M., Kuzenko, T., Jähnert, M., … Knippschild, U. (2018). Diet-Induced Obesity Affects Muscle Regeneration After Murine Blunt Muscle Trauma—A Broad Spectrum Analysis. *Frontiers in Physiology*, *9*. https://doi.org/10.3389/fphys.2018.00674

Yin, H., Price, F., & Rudnicki, M. A. (2013). Satellite Cells and the Muscle Stem Cell Niche. *Physiological Reviews*, *93*(1), 23–67. https://doi.org/10.1152/physrev.00043.2011

Zammit, P. S., Golding, J. P., Nagata, Y., Hudon, V., Partridge, T. A., & Beauchamp, J. R. (2004). Muscle satellite cells adopt divergent fates. *The Journal of Cell Biology*, *166*(3), 347–357. https://doi.org/10.1083/jcb.200312007

Zammit, P. S., Partridge, T. A., & Yablonka-Reuveni, Z. (2006). The Skeletal Muscle Satellite Cell: The Stem Cell That Came in From the Cold. *Journal of Histochemistry & Cytochemistry*, *54*(11), 1177–1191. https://doi.org/10.1369/jhc.6R6995.2006

CURRICULUM VITAE